Nigerian Research Journal of Chemical Sciences (ISSN: 2682-6054)
Volume 14, Issue 1, 2026

Metal(II) Complexes of (*E*)-4-(((2-Hydroxyethyl)imino)methyl)phenol: Synthesis, Characterization and Preliminary Antimicrobial Studies

[1]Shoetan, I. O., [2]Akeredolu, O. and *[2]Olalekan, T. E.

[1]Institute of Life Science, Swansea University (Affiliate Researcher), SA2 8PP, Wales, UK

[2]Department of Chemistry, Faculty of Science, University of Ibadan, Oyo State, Nigeria.

*Correspondence Author: topeolalekan11@yahoo.com

Accepted: *December 29, 2025.* **Published Online***: January 8, 2026*

ABSTRACT

The Schiff base ligand (HL) was synthesized from ethanolamine and 4-hydroxybenzaldehyde, and the metal complexes with Mn(II), Co(II), Ni(II), and Cu(II) were obtained in an alcoholic KOH medium. Melting point determination, FT-IR, UV–Visible, and $^{1}H/^{13}C$ NMR spectroscopies, magnetic susceptibility measurements, and metal content analysis were used to characterize the compounds. Spectroscopic data revealed that the ligand coordinates to the metal ions through the azomethine nitrogen and alcoholic oxygen atoms, forming stable chelates. Electronic spectral transitions and magnetic moment values suggested octahedral geometries for the Mn(II), Co(II), and Cu(II) complexes, while the Ni(II) complex adopted a tetrahedral configuration. The *in vitro* antimicrobial activity of the ligand and its metal complexes were evaluated against selected Gram-positive and Gram-negative bacteria, as well as fungal strains, using the agar well diffusion method. The metal complexes exhibited enhanced antimicrobial activity compared to the free ligand, with the Cu(II) complex showing the highest inhibitory effect. These findings highlight the role of metal coordination in improving the biological efficacy of Schiff base ligands and suggest potential applications of the synthesized complexes as antimicrobial agents.

Keywords: Antimicrobial activity, coordination geometry; Schiff base ligand, spectroscopic characterization, transition metal compounds

INTRODUCTION

Schiff base ligands derived from the condensation of aldehydes and amines have received sustained interest owing to their straightforward synthesis, structural flexibility, and strong propensity to form stable complexes with a broad range of metal ions. The presence of donor atoms, particularly nitrogen and oxygen, enables efficient chelation, often resulting in metal complexes with enhanced

physicochemical and biological properties [1–5]. Consequently, transition metal complexes of Schiff bases have been extensively explored for applications in catalysis, materials science, and medicinal chemistry, with notable emphasis on their antimicrobial potential. [1–2, 5–9].

The growing global threat of antimicrobial resistance, in which pathogenic microorganisms including bacteria, fungi, parasites, and viruses exhibit reduced susceptibility to conventional drugs, has intensified the search for novel antimicrobial agents with alternative mechanisms of action [10–13]. In this regard, Schiff base metal complexes offer a promising platform for drug development due to their tunable structures and diverse coordination environments [5–7].

Phenolic and alcoholic Schiff bases are particularly attractive because they possess multiple coordination sites capable of stabilizing metal ions in various oxidation states and geometrical arrangements [9,14,15]. Complexation of these ligands with first-row transition metals frequently leads to compounds with increased lipophilicity, which enhances their ability to penetrate microbial cell membranes and interact with intracellular targets [1, 3]. According to chelation theory, metal coordination reduces the overall polarity of the metal ion through partial charge sharing with donor atoms, thereby increasing the permeability of the resulting complexes through lipid layers and enhancing biological activity [16].

Although numerous Schiff base metal complexes have been reported in recent years [4—9], limited studies exist on ethanolamine-based phenolic Schiff bases derived specifically from 4-hydroxybenzaldehyde and their coordination behaviour with first-row transition metals. Furthermore, there has been no reported comparative antimicrobial data for Mn(II), Co(II), Ni(II), and Cu(II) complexes derived from the same ligand framework under identical experimental conditions. The continuous emergence of drug-resistant pathogens necessitates further exploration of new ligand frameworks and metal combinations to better understand structure–activity relationships and develop more effective antimicrobial agents.

In this context, the present study aimed to synthesise the Schiff base ligand obtained from 4-hydroxybenzaldehyde and ethanolamine, and isolate its Mn(II), Co(II), Ni(II), and Cu(II) complexes. The ligand and metal complexes were characterized using the spectroscopic, analytical, and magnetic techniques to elucidate their coordination modes, stoichiometry, and geometrical arrangements. Additionally, their *in vitro* antibacterial and antifungal activities were systematically

evaluated against elected Gram-positive and Gram-negative bacterial strains, and fungal strains to assess the impact of metal coordination on antimicrobial efficacy.

MATERIALS AND METHODS

Materials

The materials and chemicals of analytical grades were purchased from Sigma-Aldrich and used without further purification. The melting points (uncorrected) were determined using Gallenkamp melting point apparatus The IR spectra of the samples were recorded as nujol mulls on a PerkinElmer FT-IR spectrophotometer in the range 4000–350 cm^{-1}. ^{1}H and ^{13}C NMR spectra were obtained in d_6-DMSO and recorded on Bruker Avance 400 MHz NMR spectrometer; tetramethylsilane was used as the internal standard. The electronic spectra of the compounds were obtained in the UV-Vis range 400-190 nm on Labomed double beam UV-visible spectrophotometer. Percentage metal content was determined by EDTA titrimetry method. The magnetic susceptibility measurements of the metal compounds were determined on Sherwood magnetic susceptibility balance.

Synthesis of ligand and metal(II) complexes

The synthesis outline for the ligand and the Mn(II), Co(II), Ni(II) and Cu(II) complexes is shown in **Scheme 1**. Ethanolamine (2.50 g, 40.94 mmol) was added in drops to a hot methanol solution of 4-hydroxybenzaldehyde (5.00 g, 40.94 mmol) of)) while stirring and the mixture was heated to reflux for 2 h. The light brown precipitate formed was obtained by filtration, washed with diethylether, dried and weighed (4.01 g, 59%). M.p. 248-249°C; mol. wt. 165.20. ^{1}H NMR (400 MHz, DMSO-d_6): δ = 9.93 (H_a, *s*), 8.15 (H_d, *s*), 7.56 (H_c, *d, J* = 12 Hz), 6.80 (H_b, *d, J* = 12 Hz), 4.62 (H_g, *s*), 3.59 (H_f, *d, J* = 8 Hz), 3.55 (H_e, *d, J* = 8 Hz); ^{13}C NMR (400 MHz, DMSO-d_6): δ = 161.57 (C_e), 160.08 (C_a), 130.08 (C_c), 127.98 (C_d), 115.80 (C_b), 63.68 (C_f), 61.34 (C_g) ppm.

Mn(II), Co(II), Ni(II), and Cu(II) complexes were derived by mixing the appropriate metal(II) chloride (1.51 mmol) and **HL** (0.50 g, 3.03 mmol) in ethanolic KOH (0.17 g, 3.03 mmol) under refluxing conditions for 2 h. After completion, the solutions were filtered, washed, and dried to obtain the metal(II) complexes as coloured solids (Figure 1).

$[Mn(HL)_2(OH)_2]$: Brown; yield, 0.11 g (17%); mpt >360°C; $C_{18}H_{24}MnN_2O_6$, M_r, 419.34; %Mn found: 12.92, %Mn calc: 13.10. $[Co(HL)_2(OH)_2]$: Reddish-brown; yield, 0.18 g (28%); mpt >360°C; $C_{18}H_{24}CoN_2O_6$, M_r, 423.33; %Co found: 13.78, %Co calc: 13.92.

$[Ni(HL)(OH)_2].6H_2O$: Light-brown; yield, 0.18 g (33%); mpt >360°C; $C_9H_{25}NNiO_{10}$, M_r, 365.99; %Ni found: 15.22, %Ni calc: 16.04.

$[Cu(HL)_2(OH)_2]$: Green; yield, 0.40 g (54%); mpt >360°C; $C_{18}H_{24}CuN_2O_6$, M_r, 427.94; %Cu found: 14.79, %Cu calc: 14.85.

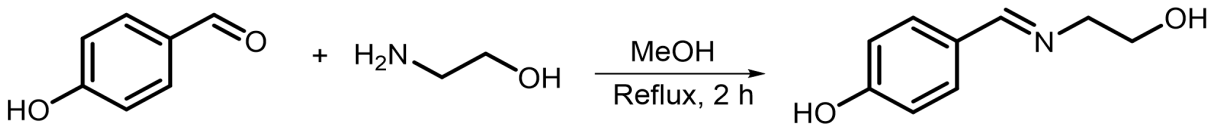

Scheme 1: Synthesis procedure for HL

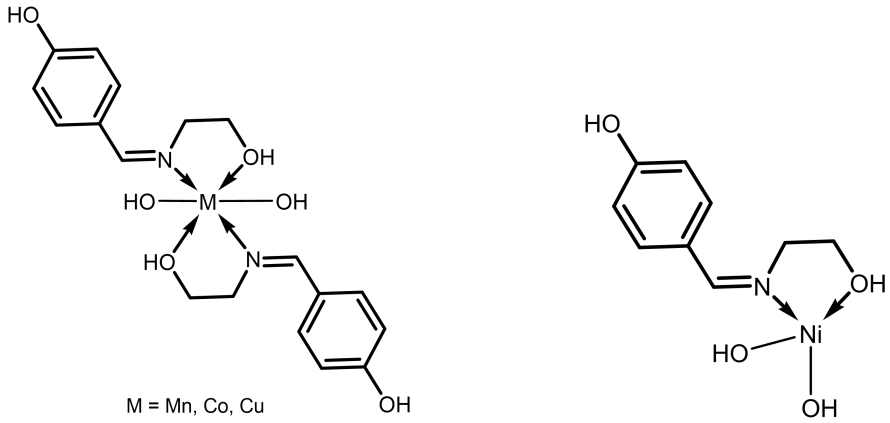

Figure 1: Metal(II) complexes of HL

In vitro antimicrobial assay procedure

The antimicrobial inhibitory potential of the derived compounds was investigated under laboratory conditions using the agar well diffusion assay. The Gram-positive *Staphylococcus aureus* (ATCC 6538) and *Bacillus subtilis* (ATCC 6633), as well as the Gram-negative *Escherichia coli* (ATCC 25922), *Pseudomonas aeruginosa* (ATCC 29853), *Salmonella typhi* (ATCC 33458), and *Klebsiella pneumoniae* (ATCC 13883) were used to test the antibacterial activity. *Candida albicans* (ATCC 10231), *Aspergillus niger* (ATCC 6275), *Penicillium notatum* (ATCC 28089), and *Rhizopus stolonifer* (ATCC 14037) were used to evaluate the antifungal efficacy.

Gentamicin at a concentration of 10 µg/mL was employed as the standard antibacterial agent, whereas tioconazole (70%) was used as the reference antifungal drug. Each compound was then

dissolved in DMSO to obtain 1 mg/mL solution, which was serially diluted to lower concentrations ranging from 500 to 31.25 µg/mL. DMSO alone served as the negative control. Microbial inocula were prepared in accordance with established microbiological protocols. The bacterial and fungal strains were respectively cultured on nutrient broth/agar and Sabouraud dextrose agar. Following solidification of the agar media, wells measuring approximately 8 mm in diameter were aseptically created, and measured volumes of the test solutions, reference drugs, and control were introduced into the wells in duplicate. Bacterial plates were incubated at 26–28 °C and examined after 24 hours, whereas antifungal activity was recorded after 48 hours of incubation [17 a,b].

RESULTS AND DISCUSSION

Analytical and spectroscopic data

The ligand and synthesized metal complexes, depicted in **Scheme 1** and Figure 1, were isolated as coloured solids. **HL** melted at 248-249 ºC while the complexes were thermally stable up to 350 ºC. The percentage metal content showed close experimental and calculated values for each metal complex.

^{1}H and ^{13}C NMR spectra

The ^{1}H and ^{13}C NMR spectra of **HL** in DMSO-d_6 are presented in Figures 2 and 3, respectively. In the ^{1}H NMR spectrum, the formation of **HL** was confirmed by the disappearance of the singlet resonance signal at approximately 10.00 ppm due to the aldehyde proton in 4-hydroxybenzaldehyde, and the appearance of a new singlet resonance signal of the imine proton at δ 8.15 ppm (H_d) [7]. The broad peaks centred at δ 9.93 and 4.62 ppm, were attributed to the phenolic (H_a) and alcoholic (H_g) protons, respectively. The azomethine (–CH=N–) proton resonated as a singlet at δ 8.15 ppm, while the aromatic protons were observed as two sets of equivalent signals at δ 7.56 (H_c) and 6.80 (H_b) ppm. The ethylene protons (–C_e–C_f–) gave doublet signals at δ 3.59 and 3.55 ppm, consistent with reported values for similar structural analogues [7,18,19].

The ^{13}C NMR spectrum exhibited a characteristic resonance for the imine carbon at δ 161.57 ppm [7]. Signals corresponding to the aromatic carbon atoms ($C_{a–d}$) were distributed within the δ 160.08–115.80 ppm range, including two pairs of equivalent carbons at δ 130.08 and 115.80 ppm. The *ipso* carbon atoms bearing the hydroxy (C_a) and imine (C_d) substituents have resonance signals at 160.08 and 127.98 ppm, respectively. The intensities of their peaks are quite unique as a result of

Nuclear Overhauser Enhancement (NOE). The ethylene carbon atoms were observed at δ 63.88 and 61.34 ppm [7].

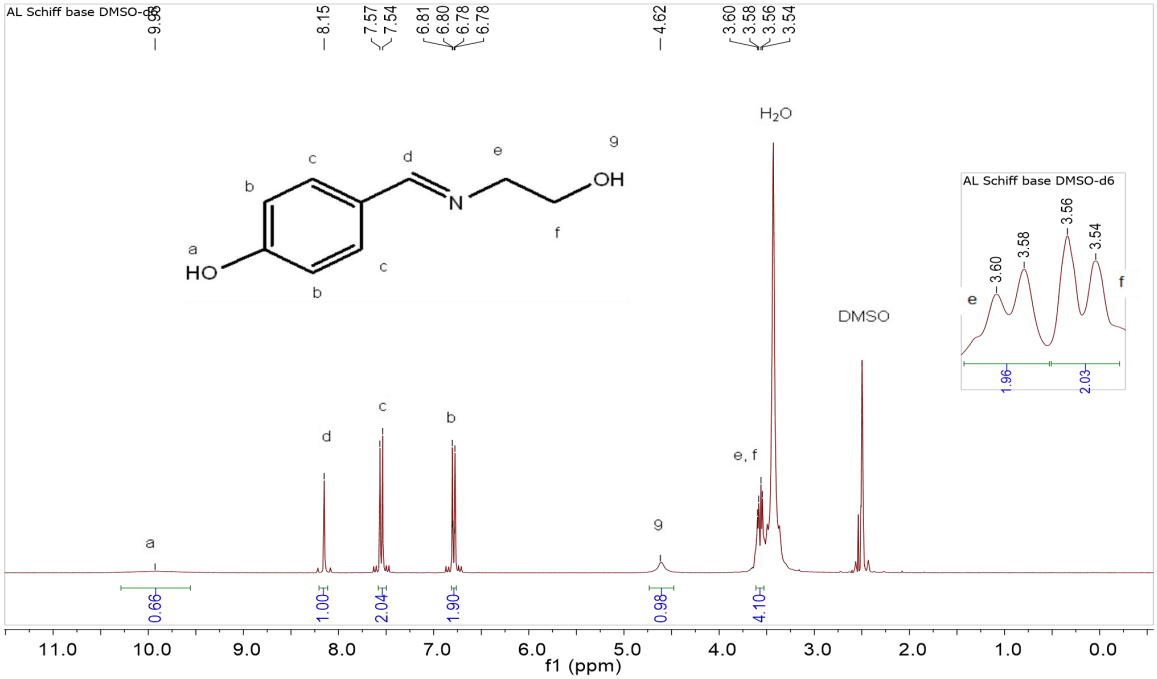

Figure 2: ^{1}H-NMR spectrum of **HL** (400 MHz, DMSO-d_6)

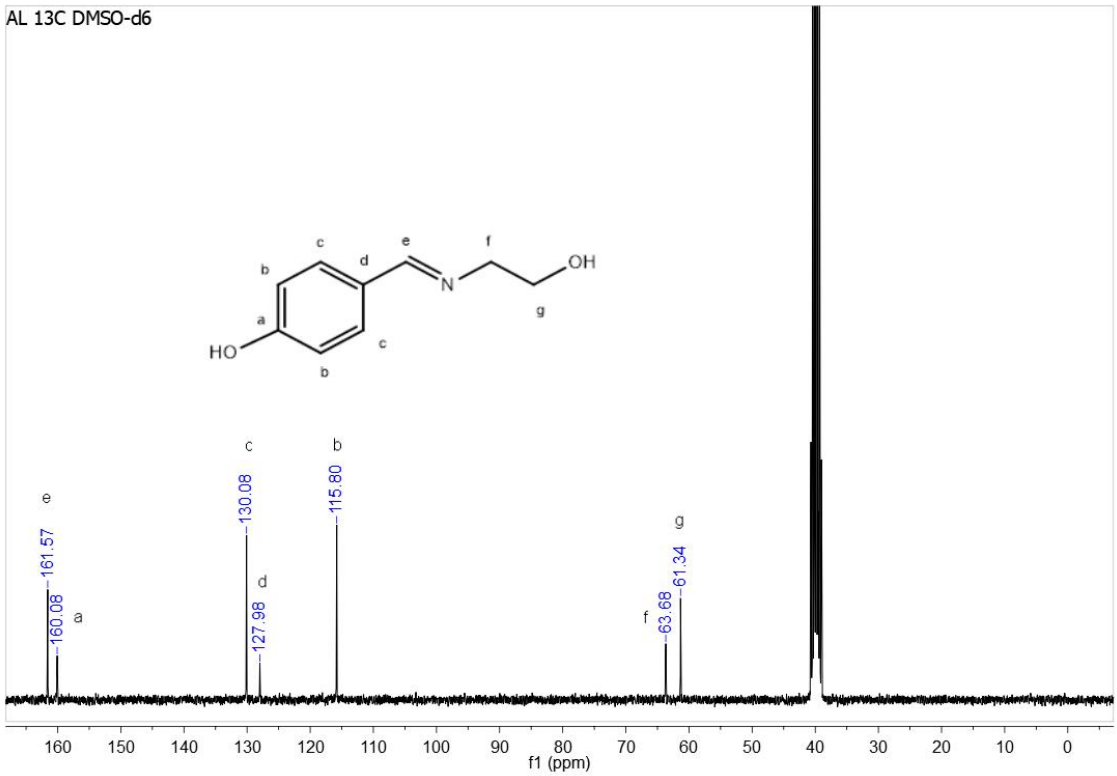

Figure 3: ^{13}C NMR spectrum of HL (400 MHz, DMSO-d_6)

Infrared spectra

The infrared spectral data of the compounds were recorded in Table 1. The weak and broad band, centered at 3071 cm^{-1}, was assigned to the alcoholic O–H vibrational frequency in the ligand **LH**. The metal complexes showed more distinct O–H stretches around 3459-3160 cm^{-1} and O-H rocking vibration, $_{\delta}$(O–H), at 611-602 cm^{-1}. These bands were ascribed to the coordinated hydroxide ion or water molecule in the metal complexes, and found to be absent in HL. The broader band observed at 3160 cm^{-1} in the spectrum of Ni(II) complex could indicate the coordination to water molecule.

In support of chelation through the alcoholic oxygen, the in-plane O–H bend and $_{\upsilon}(C–O)_{Al}$ at 1345 and 1059 cm^{-1} in HL were respectively shifted to the ranges 1354-1335 cm^{-1} and 1072-1056 cm^{-1} in the complexes. The phenolic $_{\delta}$(O–H) and $_{\upsilon}(C–O)_{Ar}$ at 1377 and 1218 cm^{-1} remained unchanged in the compounds. The aromatic ring vibrational frequencies appeared as medium bands around 1640 cm^{-1}, while those in the regions 1605–1589 cm^{-1} and 1167–1152 cm^{-1} have been attributed to the C=N and C–N stretching frequencies, respectively. The frequency shifts of 11–19 cm^{-1} suggested the imine nitrogen chelation in the metal complexes. The medium to weak vibrational frequencies, in the range 406–384 cm^{-1}, were assigned to the metal to oxygen or nitrogen coordination bands.

Table 1: Vibrational frequencies of important bands in HL and metal complexes (in cm^{-1})

Compounds / cm^{-1}	(O–H)	$_{\upsilon}$(C=C), (C=N)	$_{\upsilon}$(C–O)	$_{\upsilon}$(C–N)	$_{\upsilon}$(M–L)
HL	3071, 1377, 1345, 638	1640, 1604	1218, 1059	1166	----
$[Mn(HL)_2(OH)_2]$	3443, 1376, 616	1585	1218, 1064	1153	404, 388
$[Co(HL)_2(OH)_2]$	3459, 1377, 1339, 602	1638, 1605	1218, 1056	1167	406, 388
$[Ni(HL)(OH)_2(H_2O)]$	3337, 3160, 1377, 1335, 611	1642, 1589	1222, 1060	1152	398, 384
$[Cu(HL)_2(OH)_2]$	3449, 1377, 1354, 606	1640, 1593	1223, 1072	1154	402, 386

Electronic spectra and magnetic moments

The UV-Visible spectra and the room-temperature magnetic moments were recorded in Table 2. The electronic spectra of **HL** and the metal complexes showed $n \rightarrow \pi^*$ transitions in the range 300–362 nm. These were described as transitions between aromatic *pi* electrons and oxygen lone electrons.

Weak absorption bands arising from spin and Laporte forbidden transitions are expected from the electronic transitions associated with a Mn(II) metal centre. The electronic spectrum of $[Mn(AL)_2(OH)_2]$ displayed two absorption bands at 560 (very weak) and 486 nm (moderately weak)

which are respectively assigned to $^6A_{1g} \rightarrow {}^4T_{1g}$ and $^6A_{1g} \rightarrow {}^4T_{2g}$ transitions, in an octahedral geometry [20]. The observed magnetic moment of 4.7 BM for the present Mn(II) complex (Table 1) was lower than the spin-only value of 5.9 BM. Similar occurrence has been reported for some Mn(II) complexes with values in the range 4.3–5.8 BM [21, 22]. The lower magnetic moments were attributed to the presence of weak magnetic exchanges. The electronic spectrum of $[Co(AL)_2(OH)_2]$ features three transitions which are assigned to $^4T_{1g}(F) \rightarrow {}^4T_{2g}$ (887 nm, ν_1), $^4T_{1g}(F) \rightarrow {}^4A_{2g}(P)$ (603 nm, ν_2) and $^4T_{1g}(F) \rightarrow {}^4T_{1g}(P)$ (488 nm, ν_3) [23]. These bands are characteristic of a Co(II) centre in an octahedral geometry. The proposed octahedral geometry was supported by the effective magnetic moment of 5.2 BM obtained for the synthesized Co(II) complex, and is in alignment with the range 4.8–5.2 BM usually reported for Co(II) in an octahedral configuration [24]. Three transitions are expected to appear in the electronic spectra of tetrahedral or octahedral Ni(II) complexes, an absorption band at 660 nm observed for $[Ni(AL)_2(OH)_2]$ has been assigned to $^3T_1(F) \rightarrow {}^3T_1(P)$ (ν_3) transition in a tetrahedral geometry [25]. The other transitions, usually around 1,200 nm and 1,600 nm were not observed probably due to instrumental limit. The tetrahedral geometry of the Ni(II) complex was corroborated by the observed magnetic moment of 3.8 BM. This falls in the range of 3.7–4.0 BM expected for tetrahedral Ni(II) compounds. Effective magnetic moments in the range 2.9–3.3 BM have been reported for the octahedral geometries [24]. The observed increase to the spin-only magnetic moments of 3.87 BM for a Co(II) with 3 unpaired electrons, and 2.83 BM for Ni(II) ion with two unpaired electrons could be ascribed to the contribution to the magnetic moment due to their partly filled t_{2g} orbitals [26]. The Cu(II) complex has d^9 electronic configuration and the expected bands depend on the extent of tetragonal distortion from the ligand field, and Jahn-Teller distortion arising from non-symmetric filling of the e_g orbitals. A single band at 417 nm in $[Cu(AL)_2(OH)_2]$ can be assigned to $^2E_g \rightarrow {}^2T_g$ transition in a six coordinated Cu(II) metal centre [27, 28]. The observed magnetic moment of 2.2 BM is higher than the spin-only value (1.73 BM) for Cu(II). This is due to spin-orbit coupling as a result of mixing of the excited *T* term into the *E* ground, hence, moments of magnetically dilute compounds are in the range 1.9-2.2 BM [24].

Table 2: UV-Visible bands of HL and the metal complexes (in nm)

Compounds	$n \rightarrow \pi^*$	$d \rightarrow d$	Assignment	μ (BM)	Geometry
HL	300, 357	----	----	----	----
$[Mn(HL)_2(OH)_2]$	362	486	$^6A_{1g} \rightarrow {}^4T_{2g}$	4.7	Octahedral
		560	$^6A_{1g} \rightarrow {}^4T_{1g}$		
$[Co(HL)_2(OH)_2]$	360	488	$^4T_{1g}(F) \rightarrow {}^4T_{1g}(P)$	5.2	Octahedral
		680	$^4T_{1g}(F) \rightarrow {}^4A_{2g}(F)$		
		887	$^4T_{1g}(F) \rightarrow {}^4T_{2g}(F)$		
$[Ni(HL)(OH)_2]$	305, 354	660	$^3T_1(F) \rightarrow {}^3T_1(P)$	3.8	Tetrahedral
$[Cu(HL)_2(OH)_2]$	300, 345	417	$^2E_g \rightarrow {}^2T_{2g}$	2.2	Octahedral

Antimicrobial Activity

The diameters of inhibition zones resulting from the *in vitro* antimicrobial assay of the ligand and metal complexes are recorded in Table 3. At sample concentrations of 500 and 1000 μg/mL, HL showed activity against all the microbial strains with inhibition zones in the range 10-16 mm. $[Mn(AL)_2(OH)_2]$ exhibited activity towards all the bacteria and fungi except *Salmonella typhi and Klebsiella pneumoniae* with inhibition zones in the range 10-18 mm. Co(II) and Ni(II) compounds were active against all the microbial strains with inhibition diameters between 10 and 18 mm at 500 μg/mL, while $[Cu(AL)_2(OH)_2]$ was active against all the strains at 14-20 mm.

Table 3: The antimicrobial zones of inhibition (in mm) by **HL** and complexes

Compounds	Conc. (µg/mL)	Inhibition zone									
		Gram Positive		Gram negative				Fungi			
		S. a	*B. s*	*E. c*	*P. a*	*K. p*	*S. t*	*C. a*	*A. n*	*R. s*	*P. n*
HL	1000	16	12	14	12	12	10	12	14	12	12
	500	14	10	10	10	10	-	10	10	10	10
[Mn(**HL**)$_2$(OH)$_2$]	1000	16	18	16	18	-	-	16	14	12	14
	500	14	16	14	16	-	-	14	12	10	12
[Co(**HL**)$_2$(OH)$_2$]	1000	18	14	16	16	18	14	16	18	16	16
	500	16	12	14	14	14	12	14	14	14	14
[Ni(**HL**)(OH)$_2$].6H$_2$O	1000	18	14	16	16	14	14	16	14	14	14
	500	16	12	14	14	12	12	14	12	10	12
[Cu(**HL**)$_2$(OH)$_2$]	1000	20	20	18	18	16	16	18	16	16	16
	500	18	18	16	16	14	14	14	14	14	14
Gentamicin/Tioconazole	10	38	36	36	36	40	38	28	26	26	27
DMSO	-	8	8	8	8	8	8	8	8	8	8

CONCLUSION

A Schiff base ligand derived from 4-hydroxybenzaldehyde and ethanolamine, along with its Mn(II), Co(II), Ni(II), and Cu(II) complexes, has been successfully synthesized and characterized. Spectroscopic investigations confirmed bidentate coordination of the ligand through the azomethine nitrogen and alcoholic oxygen atoms. Infrared spectral shifts, electronic transitions, and magnetic susceptibility measurements supported octahedral geometries for the Mn(II), Co(II), and Cu(II) complexes, while the Ni(II) complex exhibited a tetrahedral structure.

The antimicrobial evaluation revealed that metal complexation enhanced the biological activity of the ligand. Among the synthesized compounds, the Cu(II) complex demonstrated the highest antimicrobial efficacy against both bacterial and fungal strains, followed by the Co(II) and Ni(II)

complexes. The improved activity of the metal complexes may be attributed to increased lipophilicity and effective metal–ligand interactions that facilitate microbial cell penetration. Overall, the results demonstrate that coordination of transition metal ions to Schiff base ligands could provide a viable strategy for developing compounds with promising antimicrobial properties.

REFERENCES

[1] Naureen, B. Miana, G. Shahid, K. Asghar, M. Tanveer, S. & Sarwar, A. (2021). Iron (III) and zinc

(II) monodentate Schiff base metal complexes: Synthesis, characterisation and biological activities,

Journal of Molecular Structure, 1231, 129946. https://doi.org/10.1016/j.molstruc.2021.129946

[2] Thakur, S. Jaryal, A. & Bhalla, A. (2023). Recent advances in biological and medicinal profile of schiff bases and their metal complexes: An updated version (2018–2023). *Results in Chemistry*, 7,

101350. https://doi.org/10.1016/j.rechem.2024.101350

[3] Sindhu, I. Singh, A. Deswal, Y. & Kirar, J.S. 2025. Exploring Schiff base ligand and their transition metal complexes: synthesis, characterization, antimicrobial, ADME and computational insight as cholesterol lowering agents and anticancer activity on HeLa cells. *Research on Chemical Intermediates*, 51, 839–873. https://doi.org/10.1007/s11164-024-05473-5

[4] Sinicropi, M.S. Ceramella. J. Iacopetta, D. Catalano, A. Mariconda, A. Rosano, C. Saturnino, C. El-Kashef, H. & Longo, P. (2022) Metal Complexes with Schiff Bases: Data Collection and Recent Studies on Biological Activities. *International Journal of Molecular Sciences*, 23(23,) 14840. https://doi.org/10.3390/ijms232314840

[5] Iacopetta, D. Ceramella, J. Catalano, A. Mariconda A. Giuzio, F. Saturnino, C. Longo, P. & Sinicropi, M.S. (2023). Metal Complexes with Schiff Bases as Antimicrobials and Catalysts. *Inorganics*, 11, 320. https://doi.org/10.3390/inorganics11080320

[6] Malav, R. & Ray, S. (2025). Recent advances in the synthesis and versatile applications of transition metal complexes featuring Schiff base ligands. *RSC Advances*, 15, 22889-22914. https://doi.org/10.1039/D5RA03626G

[7] Banan, A. Nikbakht, F. & Ataie, S. (2019). SBA-15-supported Cu (II)/Schiff-base complex as an

efficient and recyclable catalyst for one-pot azide-alkyne cycloaddition reaction. *Journal of Porous Materials*, 26, 1427–1433. https://doi.org/10.1007/s10934-019-00737-7.

[8] Ghanghas, P. Choudhary, A. Kumar, D. & Poonia, K. (2021). Coordination metal complexes with Schiff bases: Useful pharmacophores with comprehensive biological applications, *Inorganic Chemistry Communications*, 130: 2021, 108710. https://doi.org/10.1016/j.inoche.2021.108710

[9] Venkatesh, G. Vennila, P. Kaya, S. Ahmed, S.B. Sumathi, P. Siva, V. Rajendran, P. Kamal, C. (2024). Synthesis and Spectroscopic Characterization of Schiff Base Metal Complexes, Biological Activity & Molecular Docking Studies. *ACS Omega*, 9(7) 8123-8138. https://doi.org/10.1021/acsomega.3c08526

[10] WHO (2025). Global Antimicrobial Resistance and Use Surveillance System (GLASS) https://www.paho.org/en/news/13-10-2025-who-warns-widespread-resistance-common-antibiotics-worldwide. Accessed 24 December, 2025.

[11] Ventola, C.L. (2015). The antibiotic resistance crisis: part 1: causes and threats. *Pharmacology and Therapeutics*, 40(4), 277–283. PMID: 25859123

[12] Prestinaci, F. & Pezzotti, P. (2015). Pantosti, A. Antimicrobial resistance: A global multifaceted phenomenon. *Pathogens and Global Health*, 109: 309–318. https://doi.org/10.1179/2047773215y.0000000030

[13] Tacconelli, E. Carrara, E. Savoldi, A. Harbarth, S. Mendelson, M. Monnet, D. L. Pulcini, C. Kahlmeter, G. Kluytmans, J. Carmeli, Y. Ouellette, M. Outterson, K. Patel, J. Cavaleri, M. Cox, E. M. Houchens, C. R. Grayson, M. L. Hansen, P. Singh, N. Theuretzbacher, U. & Magrini, N. (2018). Discovery, research& development of new antibiotics: the WHO priority list of antibiotic-resistant bacteria and tuberculosis. *The Lancet. Infectious diseases*, 18, 318–327. https://doi.org/10.1016/S1473-3099(17)30753-3

[14] Kumar Mahto, K. & Ahmad, K. (2024). Nickel(II) and Palladium(II) complexes with imine-based

tridentate ligand: Synthesis, spectral characterization, Antimicrobial, cytotoxicity and DFT studies. *Polyhedron*, 257, 117001. https://doi.org/10.1016/j.poly.2024.117001

[15] Jorge J. Del Pino Santos K. Timóteo F. Piva Vasconcelos R.R. Ignacio Ayala Cáceres O. Juliane Arantes Granja I. de Souza D. Allievi Frizon T.E. Di Vaccari Botteselle G. Luiz Braga [16] Saba S. Rashid H. & Rafique J. (2024). Recent Advances on the Antimicrobial Activities of Schiff Bases and their Metal Complexes: An Updated Overview. *Current Medicinal Chemistry*, 31(17) 2330-2344. https://doi.org/10.2174/0929867330666230224092830.

[16] Tweedy, B.G. (1964). Plant extracts with metal ions as potential antimicrobial agents. *Phytopathology*, 55: 910–914.

[17a] NCCLS, 1999. *Methods for Determining Bactericidal Activity of Antimicrobial Agents; Approved Guideline*. NCCLS document M26-A [ISBN 1-56238-384-1]. NCCLS, Wayne, Pennsylvania 19087 USA.

[17b] NCCLS, 2002. *Reference Method for Broth Dilution Antifungal Susceptibility Testing of Yeasts; Approved Standard—Second Edition*. NCCLS document M27-A2 (ISBN 1-56238-469-4). NCCLS, Wayne, Pennsylvania 19087-1898 USA, 2002.

[18] Turecka, K. Chylewska, A. Kawiak, A. & Waleron, K.F. (2018). Antifungal Activity and Mechanism of Action of the Co(III) Coordination Complexes With Diamine Chelate Ligands Against Reference and Clinical Strains of *Candida* spp. *Frontiers in microbiology*, 9, 1594. https://doi.org/10.3389/fmicb.2018.01594.

[19] Akeredolu, O. Adebusuyi, F.O. Adebayo-Tayo, B.C. & Olalekan, T.E. (2025). Synthesis and Antimicrobial Activity of Nitrobenzaldehyde Schiff base and Complexes. *Nigerian Journal of Chemical Research*, 29(2), 062–072. https://doi.org/10.4314/njcr.v29i2.1

[20] Chandra, S. and Sharma, S.D. (2002). Cr(III), Mn(II), Co(II), Ni(II), Cu(II)& Pd (II) complexes of 12 memberd tetraaza (N4) macrocyclic ligand. *Transition Metal Chemistry*, 27, 732-735. http://dx.doi.org/10.1023/A:1020309322470

[21] Drzewiecka-Antonik, A. Ferenc, W. Mirosław, B. Osypiuk, D. & Sarzyński, J. (2021). Structure,

thermal stability and magnetic behavior of Mn(II) complexes with phenoxyacetic acid herbicides.

Polyhedron, 207, 115370. https://doi.org/10.1016/j.poly.2021.115370

[22] Batra, G. & Mathur, P. 1994. Mononuclear and binuclear manganese(II) complexes with tridentate *bis*-benzimidazolyl ligands. *Transition Metal Chemistry*, 19, 160–164. https://doi.org/10.1007/BF00161880

[23] Pervaiz, M. Ahmad, I. Yousaf, M. Kirn, S. Munawar, A. Saeed, Z. Adnan, A. Gulzar, T. Kamal, T. Ahmad, A. & Rashid, A. (2019). Synthesis, spectral and antimicrobial studies of amino acid derivative Schiff base metal (Co, Mn, Cu & Cd) complexes. *Spectrochimica Acta Part A: Molecular and Biomolecular Spectroscopy*, 206, 642-649. https://doi.org/10.1016/j.saa.2018.05.057.

[24] Greenwood, N.N. & Earnshaw, A. (1998). *Chemistry of the Elements 2nd Edition*. Butterworth-Heinemann, United Kingdom. https://doi.org/10.1016/C2009-0-30414-6

[25] Abdel Aziz, A.A. & Seda, S.H. (2017). Synthesis, Spectral Characterization, SEM, Antimicrobial, Antioxidative Activity Evaluation, DNA Binding and DNA Cleavage Investigation of Transition Metal(II) Complexes Derived from a tetradentate Schiff base bearing thiophene moiety. *Journal of Fluorescence*, 27, 1051–1066. https://doi.org/10.1007/s10895-017-2039-9

[26] Housecroft, C.E. & Sharpe, A.G. (2012). *Inorganic Chemistry 4th Edition*. Pearson Education Limited, England.

[27] Abdel-Rahman, L.H. Abu-Dief, A.M. Aboelez, M.O. & Hassan Abdel-Mawgoud, A.A. (2017). DNA interaction, antimicrobial, anticancer activities and molecular docking study of some new VO(II), Cr(III), Mn(II) and Ni(II) mononuclear chelates encompassing quaridentate imine ligand. *Journal of photochemistry and photobiology. B, Biology*, 170, 271–285. https://doi.org/10.1016/j.jphotobiol.2017.04.003

[28] Olalekan, T.E. Adejoro, I.A. VanBrecht, B. & Watkins, G.M. (2015). Crystal structures, spectroscopic and theoretical study of novel Schiff bases of 2-

(methylthiomethyl)anilines. *Spectrochimica acta. Part A, Molecular and biomolecular spectroscopy*, 139, 385–395. https://doi.org/10.1016/j.saa.2014.12.018